Title
Effect of random and scatter fractions in variance reduction using time-of-flight information

Authors
Kimdon, Joey A.
Qi, Jinyi
Moses, William W.

Publication Date
2003-05-23

Effect of Random and Scatter Fractions in Variance Reduction using Time-of-Flight Information

Joey A Kimdon*, Jinyi Qi†, William W Moses†
*University of California, Berkeley
†Ernest Orlando Lawrence Berkeley National Laboratory, Berkeley, CA 94720

***Abstract*— The ability of differential time-of-flight (TOF) information to reduce the statistical noise variance in PET reconstructions has been known since the 1980's. Since then, the technology and applications of PET have evolved, warranting a reconsideration of the estimated improvements of TOF with respect to modern PET. For example, whereas 2D cardiology or neurology studies were once the only options, 3D clinical whole-body oncology imaging is becoming more common. The augmented sensitivity, change in object size and shape, as well as the accompanying changes in isotope and dose, result in different relative amounts of scattered, random, and true coincidences than were seen in the past. Thus in an analysis of the TOF gain for modern PET, it is useful to consider the separate effects of varying these fractions. We present a simulation study investigating the relative amount of TOF contrast-to-noise gain for a range of levels of scattered and random coincidences. We demonstrate that both increased scatter and increased randoms noticeably enhance the TOF gain, but that the higher randoms fraction introduces the most drastic improvement. These results are encouraging for modern PET, where there is a greater random/scatter fraction than in the PET of the 1980's.**

I. Introduction

In the early 1980's, techniques and technology were developed to utilize differential time-of-flight (TOF) information for reconstructing positron emission tomography (PET) images. Timing information reduces the possible position of a single coincidence event from the entire chord along the line of response to a line segment centered around the perceived site of annihilation. Since the signal to noise ratio of a reconstructed image depends on this range [1], TOF improves the statistical noise properties of reconstructed PET images. Mathematical formulations, simulations, and experiments were made in the context of backprojection [2]–[5], maximum likelihood [6]–[9], and extended to 3D [11], [12]. Another advantage is the ability to reject random coincidences outside the field of view in a manner similar to a hardware timing window but with a potentially shorter window width [10].

Although the image quality improvements were attractive, TOF was not viable at the time. The characteristics of the scintillation materials available in the early 1980's had either poor timing resolution (e.g. BGO at approximately 6 ns, which corresponds to 90 cm of positioning error from the center of the field of view – much too large to be useful for a human body) or an undesirable trade-off between spatial resolution and detector efficiency due to a longer attenuation length (e.g. BaF_2 and CsF), so research in TOF drastically decreased by the 1990's. Recently, there has been renewed interest in using LSO [13] or $LaBr_3$ [14] to achieve timing accuracy of approximately 500 ps while maintaining other attractive properties for PET, such as short attenuation length, fast decay time, and high light output, bringing TOF PET back into consideration as a feasible technique. As LSO scintillators are being integrated into commercially produced PET machines, the transition to TOF is becoming more practical.

With the renewed interest in TOF, we wish to reconsider the analysis of the estimated image quality improvement in the context of modern PET. PET technology and applications have developed in the last 20 years, and many of these changes affect the performance of the TOF technique. For instance, applications go beyond 2D cardiology and neurology to include frequent clinical whole-body 3D oncology imaging, and isotope choice has migrated from ^{15}O or ^{13}N to favor ^{18}F, leading to different administered doses. These changes affect the fraction of detected random and scattered coincidences with respect to true detected events, and each of these distinct noise phenomena could potentially alter the expected TOF performance, so it is useful to consider them individually in the TOF analysis. The formulation of the noise equivalent count rate [15], which is yet another development in the last 15 years, is a measure which allows the comparison of the separate effects of randoms and scatter, making TOF analysis of the individual components a reasonable goal. The simulations reported in this abstract aim to identify the expected TOF variance reduction effects at different levels of random and scattered coincidences, similar to the levels found in modern PET studies (i.e. whole body, FDG, oncology.)

II. Methods

The simulation and reconstruction program was adapted from in-house list-mode likelihood code described in [16]. Timing information was generated assuming a Gaussian distribution with FWHM (full width at half maximum) of 500 ps around the correct arrival time difference. Then the contribution to the system matrix for each event changed from a flat distribution

This work was supported by the Director, Office of Science, Office of Biological and Environmental Research, Medical Sciences Division of the U.S. Department of Energy under contract DE-AC03-76SF00098 and by Public Health Service Grants Nos P01-HL25840 and R01-CA67911.

(for standard PET) to a Gaussian centered around the position estimate.

The detector ring in the simulations has a diameter of approximately 80cm, and utilizes large detectors (1cmx1cmx3cm) and a fairly course resolution (1 cm) to reduce computation time and storage space. True events arise from a 35 cm diameter uniform circular distribution and a 1 cm diameter bright internal circle with an intensity ratio of about 6:1 compared with the background. The number of true events was held constant at about 40,000. The simulation was done in 2D. Scattered events were modeled with a radially symmetric Gaussian distribution with a FWHM of 35 cm. Randoms were modeled by uniformly populating detectors and selecting a time difference from a uniform distribution within a coincidence window width of 12 ns. Random and scatter fractions were controlled manually by adding coincidences in true:noise ratios of 1:0, 4:1, 2:1, and 1:1. Events interacting in crystals separated by less than $1/3$ of the total number of detectors in the ring were discarded in both TOF and standard tomographic simulations and not counted in the above ratios. Attenuation was not modeled, and random/scatter correction was not performed. Images were reconstructed with 100 iterations by a preconditioned conjugate gradient ML algorithm.

III. Results

In Fig. 1 we compare the contrast to noise ratios (CNR) of the resulting reconstructions, where CNR is calculated as $(H - B) / (B\sigma_B)$, where H is the mean of the bright center spot, B is the mean within the background, (i.e. within the 35 cm circle but external to the hot spot) and σ_B is the spatial standard deviation of the background. The ordinate represents the ratio of the CNR using TOF to that of standard PET, and the abscissa indicates an increasing fraction of false coincidences, either randoms or scatter depending on the curve in question. We can clearly see that the improvement in image quality with TOF increases with the addition of scattered events and even more so with respect to random coincidences, particularly with higher random/scatter fractions. Since these are not true coincidences, the placement of isotope concentration they cause will not be consistent with the rest of the data, and since TOF positions these events more accurately, it is reasonable that TOF would reduce their effect. In addition, the improvement seen with increased randoms also includes an effect similar to a reduction of the coincidence window, for the Gaussian falloff minimizes the contribution from events outside the field of view. The improved quality is visible in sample reconstructions, as seen in Fig. 2. The greater benefit of TOF when we consider randoms and scatter is promising for modern PET, which exhibits more scatter and random coincidences than the PET of the 1980's.

Future work will include more realizations with a finer sampling and a wider range of noise:true fractions to more precisely determine the nature of the CNR ratio curves in Fig. 1. In the case of randoms, to better characterize the improvement beyond the effective coincidence window reduction, we will run simulations where we reject randoms outside the 35 cm circle for both TOF and non-TOF simulations. We will also experiment with different timing and spatial resolutions, overall counts, and the effect in 3D.

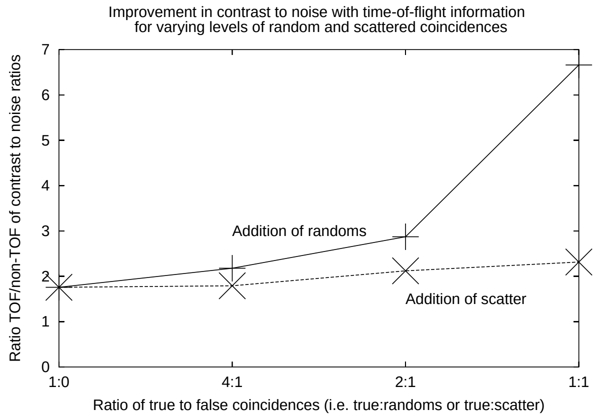

Fig. 1. CNR comparison between TOF and standard PET. Increased random or scatter fractions show a significant increase in the image quality improvement obtained with TOF.

IV. Acknowledgment

This work was supported by the Director, Office of Science, Office of Biological and Environmental Research, Medical Sciences Division of the U.S. Department of Energy under contract DE-AC03-76SF00098 and by Public Health Service Grants Nos P01-HL25840 and R01-CA67911.

V. Disclaimer

References

[1] Budinger TF, Derenzo SE, Greenberg WL, Gullberg GT. Quantitative Potentials of Dynamic Emission Computed Tomography. *J Nucl Med* 19(3):309-315, 1978.

[2] Snyder DL, Thomas LJ Jr, Ter-Pogossian MM. A Mathematical Model for Positron-Emission Tomography Systems having Time-of-Flight Measurements. *IEEE Trans Nucl Sci* 28(3):3575-3583, 1981.

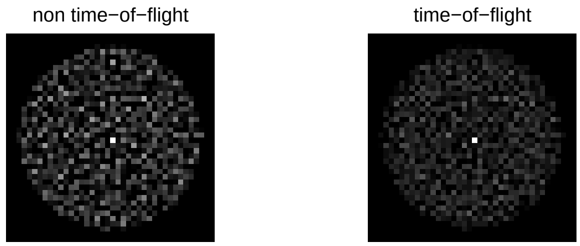

(a) Only true coincidences

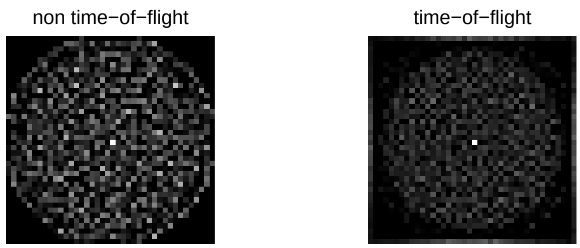

(b) True:scatter ratio = 1:1

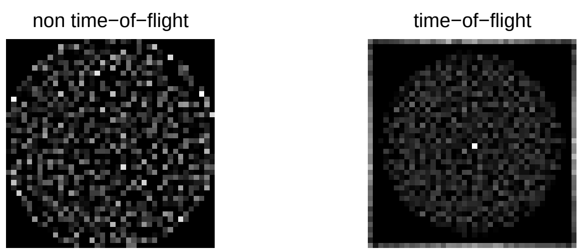

(c) True:random ratio = 1:1

Fig. 2. Image quality improvement due to TOF is visible in these sample reconstructions. The simulated distribution is a single bright 1 cm diameter circle (= 1 pixel) in the center of a 35 cm diameter circle. The activity density in the bright spot is 6 times that of the large circle.

[3] Tomitani T. Image Reconstruction and Noise Evaluation in Photon Time-of-Flight Assisted Positron Emission Tomography. *IEEE Trans Nucl Sci* 28(6):4582-4589, 1981.

[4] Tanaka E. Line-writing data acquisition and signal-to-noise ratio in time-of-flight positron emission tomography. *IEEE Workshop Time-of-Flight Tomog* May:101-108, 1982.

[5] Budinger TF. Time-of-Flight Positron Emission Tomography: Status Relative to Conventional PET. *J Nucl Med* 24(1):73-78, 1983.

[6] Politte DG, Snyder DL. Image reconstruction from list-mode data in an emission tomography system having time-of-flight measurements. *IEEE Trans Nucl Sci* NS-20(3):1843-1849, 1983.

[7] Politte DG. Image improvements in positron-emission tomography due to measuring differential time-of-flight and using maximum-likelihood estimation. *IEEE Trans Nucl Sci* 37(2):737-742, 1990.

[8] Barrett HH, Parra L, White T. List-mode likelihood. *J Opt Soc Amer* 14(11):2914-2923, 1997.

[9] Parra L, Barrett HH. List-mode likelihood: EM algorithm and image quality estimations demonstrated on 2-D PET. *IEEE Trans Med Imag* 17(2):228-235, 1998.

[10] Yamamoto M, Hoffman GR, Ficke DC, Ter-Pogossian MM. Imaging algorithm and image quality in time-of-flight assisted positron computed tomography: Super PETT I. *IEEE Workshop on Time-of-Flight Tomography* May:125-129, 1982.

[11] Mallon A, Grangeat P. Three-dimensional PET reconstruction with time-of-flight measurement. *Phys Med Biol* 37(3):717-729, 1992.

[12] Mallon A, Grangeat P, Thomas PX. Comparison between three-dimensional positron emission tomography with and without time-of-flight measurement. *Conf Record. IEEE Nucl Sci Symposium and Med Imag Conf* 2:988-990, 1992.

[13] Moses WW, Derenzo SE. Prospects for Time-of-Flight PET using LSO Scintillator. *IEEE Trans Nucl Sci* 46(3):474-478, 1999.

[14] Surti S, Karp JS, Muehllehner G, Raby PS. Investigation of Lanthanum Scintillators for 3D PET. *Conf Record. IEEE Nucl Sci Symposium and Med Imag Conf* 2002.

[15] Strother SC, Casey ME, Hoffman EJ. Measuring PET scanner sensitivity: Relating count rates to image signal-to-noise ratios using noise equivalent counts. *IEEE Trans Nucl Sci* NS-37:783-788, 1990.

[16] Huesman RH, Klein GJ, Moses WW, Qi J, Reutter BW, Virador PRG. List-Mode Maximum-Likelihood Reconstruction Applied to Positron Emission Mammography (PEM) with Irregular Sampling. *IEEE Trans Med Imaging* 19(5):532-537, 2000.